Electron Microscopy Study of the Aging and First Stage of Tempering of High-Carbon Fe-C Martensite

O.N.C. UWAKWEH, J.-M.R. GÉNIN, and J.-F. SILVAIN

Transmission electron microscopy (TEM) observations of 1.95 wt pct C martensite samples, aged at 330 and 352 K for 1 and 2 hours, respectively, confirm the fact that the two steps of aging, as evidenced by Mössbauer spectroscopy kinetics study, are due to clustering and subsequent long-range ordering. Streaks are observed along $\langle 203 \rangle^*$ directions during clustering, and in addition, two types of split superstructure spots appear during ordering at the advanced stage of aging. These are tentatively explained by a 1C-2Fe-1C-5Fe-1C-5Fe sequence of carbon and iron atoms arranged along $[001]_{\alpha'}$, which gives rise to antiphase domains with a $12a$ superperiod within the alternating carbon-rich and carbon-depleted regions, where a is the lattice parameter of body-centered cubic (bcc) iron. The associated formula is Fe_6C. In the first stage of tempering, the orthorhombic structure of the precipitated carbide is confirmed, while evidence of ordering as in Co_2N is lacking. The Fe_9C_4 stoichiometry, which is close to the experimental $Fe_{2.4}C$, is instead proposed for ε- or η-carbide.

I. INTRODUCTION

IF the tempering of martensite is now understood, aging phenomena occurring at temperatures lower than those at which tempering occurs and known under the generic name of aging still constitute a very active field of interest, as is testified by several recent contributions.[1–7] All of these studies converge on the general idea that there exists a continuous redistribution of the carbon interstitials which starts at a temperature as low as about 200 K and which evolves into the *in situ* precipitation of the ε- or η-carbide observed during the first stage of tempering.

This study accompanies that of the kinetics of aging and of the first stage of tempering of high-carbon martensite investigated by Mössbauer spectroscopy[7] (Figure 1). Several electron microscopy observations have been made, among which those of Nagakura and co-workers[8–12] or Taylor and co-workers[4,5,6] are presently the most exhaustive. The experimental information reported in our study does confirm most of their previous findings. However, the present work will clarify several specific salient points which are not yet well settled.

The kinetic study quoted above[7] allows for the determination of the most suitable heat treatment for attaining a given stage of aging or tempering. Moreover, by using only high-carbon binary alloys, one discards any confusion which might exist in ternary Fe-Ni-C alloys where nickel could affect the aging and tempering behavior.[4,5,6] Besides the fact that it obviously enhances and thus facilitates the observations, high carbon content prevents the complications that could arise due to high M_s (martensite start) temperature inherent with low-carbon alloys.

O.N.C. UWAKWEH is a former Graduate Student of the University of Nancy and Laboratoire CNRS Maurice Letort. J.-M.R. GÉNIN, Professor and Department Head, and J.-F. SILVAIN, Research Scientist, are with the Department of Materials Science, University of Nancy, ESSTIN and the Laboratoire CNRS Maurice Letort, Parc R. Bentz, 54500 Vandoeuvre, France.

Manuscript submitted March 14, 1990.

II. EXPERIMENTAL

Sample preparation carefully follows the procedure already described for the kinetics study.[7] Several of the samples are actually those already used for the Mössbauer investigation, and the others are prepared exactly the same way. Therefore, one can insure that the microscopy observations correlate with the phenomena revealed from Mössbauer spectroscopy, which describes the statistical distribution of the environments of the iron nuclei. Thus, samples are made of 80-μm-thick ARMCO* iron foils carburized at 1140 °C in a $1/5CH_4$-H_2 gas mixture, for obtaining about 1.95 wt pct C, and quenched at room temperature, where the samples are 100 pct retained austenite. The M_s temperature of this type of alloy is below 235 K. Then, after a second quench to 78 K is carried out, up to 60 pct of the austenite transforms to the martensitic phase α', as evidenced from Mössbauer spectral analysis. Aging or tempering heat treatment follows before room-temperature thinning, and the TEM observation is made with a microscope operated at 80 or 200 kV and equipped with a tilt stage.

*ARMCO is a trademark of Armco, Inc., Middletown, OH.

III. RESULTS

A. *General*

The morphology displays the classical features of high-carbon steels, as illustrated in Figure 2(a). Martensitic crystals are platelike with a $\{259\}_\gamma$ habit plane, as usual for high carbon content with high tetragonality.[13] Plates of different sizes originating from a common area in the austenite grain and intersecting one another are easily observed. These facts suggest that the martensitic transformation here is burst type in character. The contrast lying along the plate in its middle, known as the midrib zone, is clearly seen in each plate. Two types of twins are observed:[5,14] $\{112\}_{\alpha'}$ twins abound around the midrib zone, and $\{011\}_{\alpha'}$ twins are more likely seen close to the α'/γ interface (Figure 2(b)).

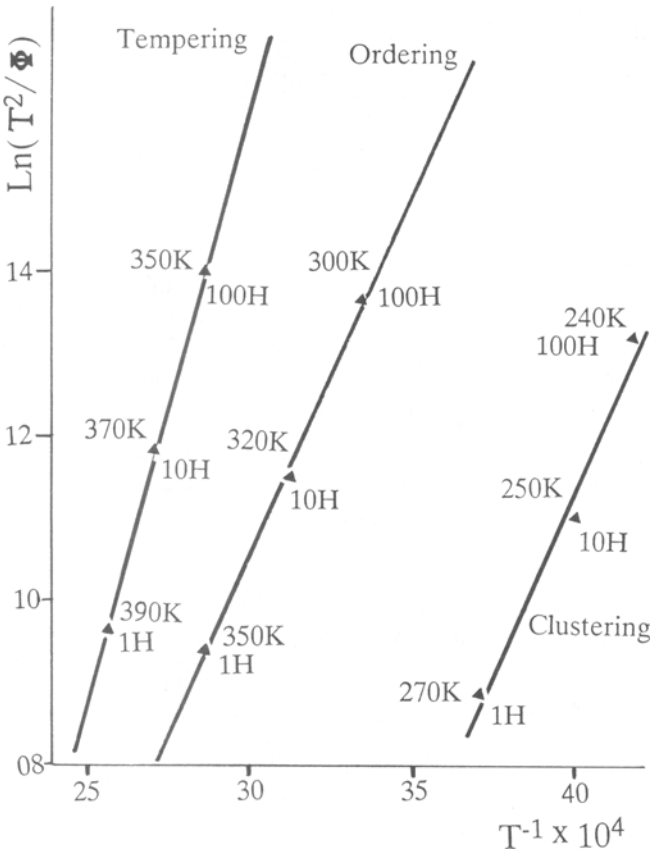

Fig. 1—Kinetics of the two steps of aging and first stage of tempering of a 1.95 wt pct C iron martensite as determined from Mössbauer spectroscopy by isochronal holdings of 1, 10, and 100 h at 10 K intervals.[7] Clustering and ordering correspond to 75 kJ/mole and tempering to 121.5 kJ/mole.

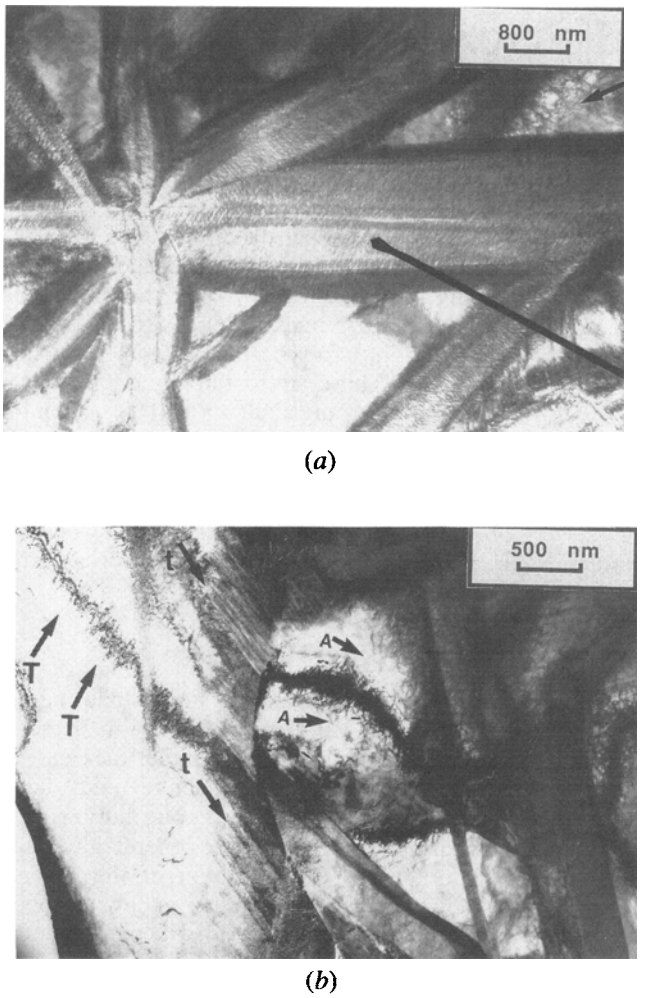

Fig. 2—(*a*) Morphology of the 1.95 wt pct C iron sample, displaying the martensite plates with $(259)_\gamma$ habit plane in the austenite matrix. (*b*) The two twinning modes in the martensite, "t" and "T", *i.e.* $(112)_{\alpha'}$ and $(011)_{\alpha'}$, and the dislocation network in the austenite ("A").

The primary $\{112\}_{\alpha'}$ twinning mode, which exists in cubic iron as well as in tetragonal martensites, originates from those $\{101\}_\gamma$ planes in the austenite matrix which bisect the future tetragonal axis before Bain distortion,[5,14] and two twin-related regions within a given martensite plate have the same Bain axis. The $\{011\}_{\alpha'}$ twinning mode concerns only those planes in the tetragonal structure which are not mirror planes. They originate from the $\{111\}_\gamma$ planes and have been observed in 1.82 wt pct C binary alloy.[14] Since $\{011\}_{\alpha'}$ twinning only exists in martensites of high tetragonality, it is not a common transformation mode and is taken to result from post-transformation effects which relieve large stresses and strains.[5,14] For low-carbon steels, these accommodation $\{011\}_{\alpha'}$ twins are replaced by dislocations at the periphery of the α' crystals. In the alloys used in this study (>1.8 wt pct C), dislocations of any form have never been observed, even at the highest resolution in the α' phase. In the retained austenite, a high density of dislocations is found close to the γ/α' interface, as designated by arrows in Figures 2(a) and (b). They originate from the accommodation strain in the vicinity of martensite plates.

B. *Aging of Martensite*

The kinetic study based on Mössbauer spectroscopy,[7] which is illustrated in Figure 1, displays during the aging process two different steps that we attributed to the clustering of carbon atoms into "isolated multiplets" followed by the coarsening of carbon-rich regions due to the ordering of multiplets into "extended multiplets."[1] That study showed clearly that the activation energy (75 kJ/mole) is the same for the two steps of aging and matches the migration energy of carbon in martensite. One carefully distinguishes the "isolated multiplet," which consists of one small chain of carbon atoms lying along an overall $\langle 011\rangle_{\alpha'}$ direction and made of basic C-C $1/2\langle 111\rangle_{\alpha'}$ pair configurations, from the "extended multiplet," which is its extension by ordering and consists of parallel $\langle 011\rangle_{\alpha'}$ multiplets separated by $\langle 020\rangle_{\alpha'}$ vectors.[1,3] From the kinetics information,[7] two different heat treatments are carried out in this study. The first one corresponds to isochronal holdings from the as-quenched state to 330 K at 10 K intervals for 1 hour. According to Figure 1, the clustering step for isochronal holdings of 1 hour starts at 270 K, whereas the ordering step has completely evolved at 350 K. Thus, 330 K seems reasonable for reaching an advanced stage of clustering

before ordering occurs. The second heat treatment is done from the same bulk sample, which is then treated for two more hours at 352 K to insure a complete ordering.

A typical diffraction pattern of the sample aged at 330 K is shown in Figure 3(a), where the incident beam is parallel to $\langle 111 \rangle_{\alpha'}$, accompanied by its corresponding bright-field image (Figure 3(b)). Diffuse scattering streaks about the fundamental spots elongating approximately along the $\langle 101 \rangle^*$ directions of the reciprocal space are easily seen. The extremities of the streaks are more intense, leading sometimes to the belief that they were mere satellites.[11,12] These features have also been reported in the studies of the early stage of aging[4,15,16] and explained in Reference 17. In particular, Taylor *et al.*[4] concluded that the actual direction of the streaks is, in fact, closer to $[203]^*$ than $[101]^*$. The bright-field image of Figure 3(b) shows the tweedlike structure modulation which corresponds to two variants of the carbon-rich regions.

The diffraction patterns of the sample aged at 352 K are displayed in Figure 4. Three incident beams are used, $\langle 100 \rangle_{\alpha'}$, $\langle 110 \rangle_{\alpha'}$, and $\langle 111 \rangle_{\alpha'}$, in order to construct completely the reciprocal lattice (Figure 4(d)). Besides the diffuse scattering streaks observed at lower temperature, one notes the appearance of superstructure spots. These spots can be classed into two sets. One set looks like split spots along the $[001]^*$ direction, with a split distance of $(1/6)2\mathbf{c}^*$ around fundamental spots (h, k, l) such that $(h + k + l)$ is odd. This set is uniquely visible in Figure 4(a), *i.e.*, the $[010]_{\alpha'}$ pattern. Another set looks like split spots along $[001]^*$, with a split distance of $(1/12)2\mathbf{c}^*$ around spots $(h/2, k/2, l)$. Figure 4(b), *i.e.*, the $[1\bar{1}0]_{\alpha'}$ pattern, displays both types of spots and strongly resembles Figure 7 of Reference 12. In particular, the $(1/6)2\mathbf{c}^*$ splitting of (001) and $(1/12)2\mathbf{c}^*$ splitting of $(1/2, 1/2, 0)$ and $(1/2, 1/2, 1)$ reflections are easily seen. Finally, Figure 4(c), *i.e.*, the $[1\bar{1}1]_{\alpha'}$ pattern, displays only split spots of the $(1/12)2\mathbf{c}^*$ type. Because the split spots are slightly off the $(1\bar{1}1)^*$ plane, they look like a dash elongating along the $[\bar{1}12]^*$ direction. Figure 4(d) represents the three-dimensional reciprocal lattice. This study definitively confirms the experimental observation made by Nagakura and Toyoshima.[10]

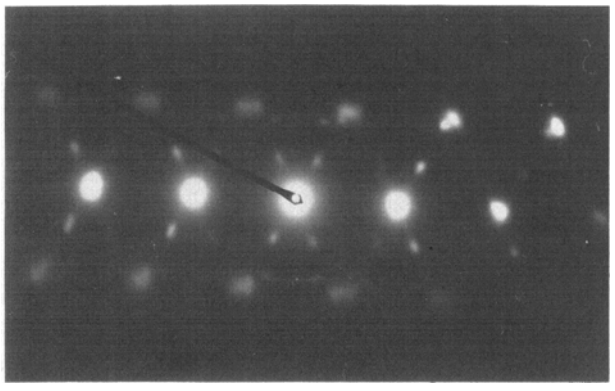

(*a*)

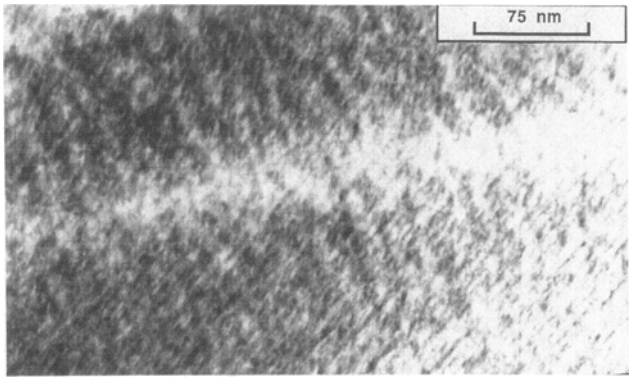

(*b*)

Fig. 3—Sample aged from as-quenched state to 330 K by isochronal holdings at 10 K intervals for 1 h: (*a*) diffraction pattern with incident beam parallel to $[111]_{\alpha'}$, displaying diffuse scattering streaks, and (*b*) bright-field electron micrograph, showing the tweedlike structure modulation of the martensite.

The morphology of the fully aged martensite is illustrated by the bright- and dark-field micrographs of Figures 4(e) and (f). The first one was taken at high resolution in the $[1\bar{1}0]_{\alpha'}$ orientation of Figure 4(b) and presents the precipitates corresponding to the dark areas. These are aligned and alternate with clearer areas representing the carbon-depleted matrix. One variant of the precipitates is exhibited here. The dark-field micrograph is taken with one of the superstructure spots in the $[010]_{\alpha'}$ orientation of Figure 4(c). Tiny needlelike precipitates are seen scattered uniformly in the matrix, except in the midrib zone close to the center of the micrograph. These general features have been described by Grégoire *et al.*[18] as a "pepper and salt" contrast observed in a transmission electron microscopy (TEM) study of aged Fe-Ni-C alloys.

C. *First Stage of Tempering*

From the kinetics calibration of Figure 1, the first stage of tempering has completely replaced the aging processes at 390 K for 1-hour isochronal holdings. The experimental results presented here are obtained from the very sample used for the Mössbauer study[7] which was isochronally treated for 1 hour up to 450 K. A bright-field micrograph centered about the midrib zone shows, in Figure 5(a), the crisscross contrast due to two different platelike carbide variants with a $\{102\}_{\alpha'}$ habit plane in conformity with the observation of Taylor *et al.*[6] Figures 5(b) through (g) are the diffraction patterns and key diagrams corresponding to the incident beam parallel to the matrix directions $[100]_M$, $[001]_M$, $[\bar{1}11]_M$, $[11\bar{1}]_M$, $[\bar{1}13]_M$, and $[\bar{3}13]_M$, respectively.

IV. DISCUSSION

Emphasis will be placed on the interpretation of the experimental results we present and, more precisely, on the description of the structures of the ordered carbon-rich regions for aging and of the carbide precipitates for the first stage of tempering.

A. *The Ordered Aged Structure*

If the early stage of aging has been fully investigated,[4,11,12,15,16] one notes that only Nagakura and coworkers[10,12] have obtained diffraction patterns of the same

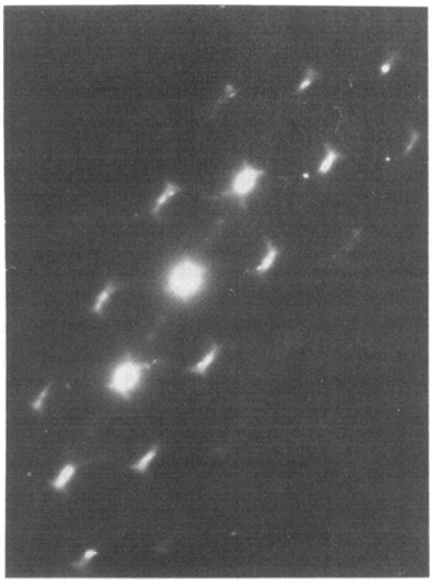

(a)

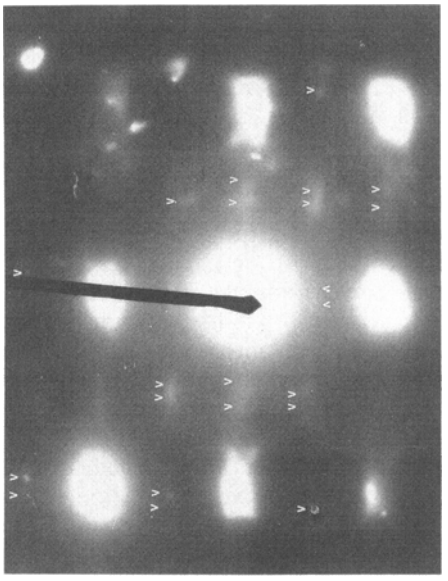

(b)

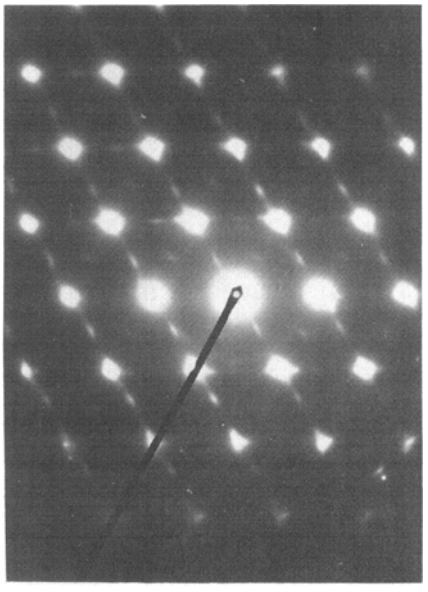

(c)

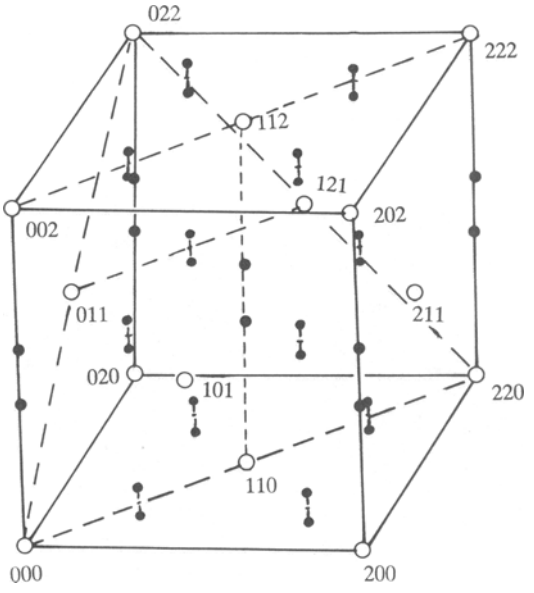

(d)

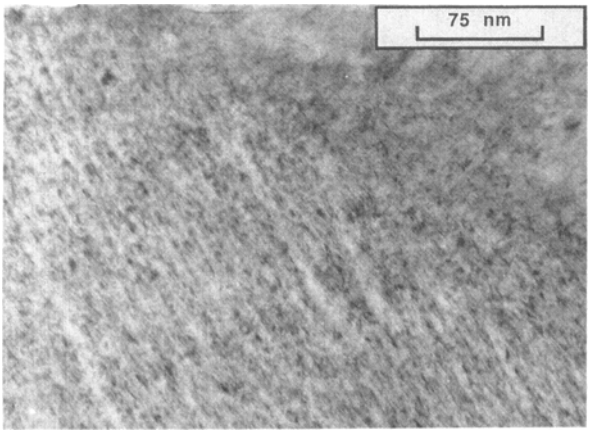

(e)

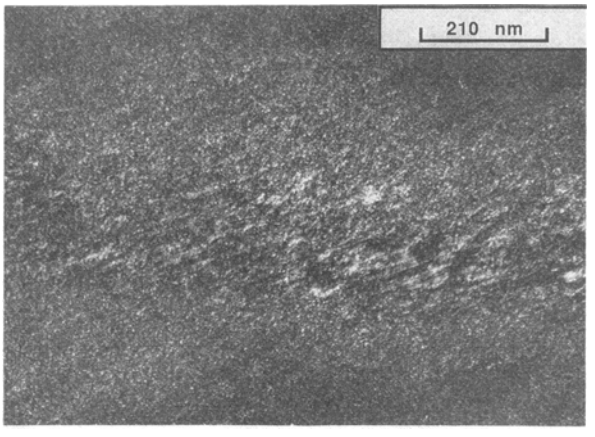

(f)

Fig. 4—Sample aged as that of Fig. 3, with additional aging at 352 K for 2 h: (*a*) diffraction pattern with beam $\parallel [100]_{\alpha'}$, (*b*) $\parallel [1\bar{1}0]_{\alpha'}$, (*c*) $\parallel [1\bar{1}1]_{\alpha'}$, (*d*) three-dimensional reciprocal lattice, (*e*) bright-field electron micrograph of (b) at high resolution, and (*f*) dark-field image taken with one superstructure spot of (a).

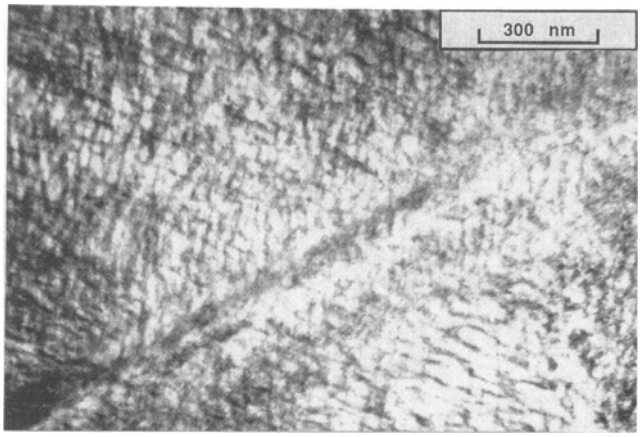

(*a*)

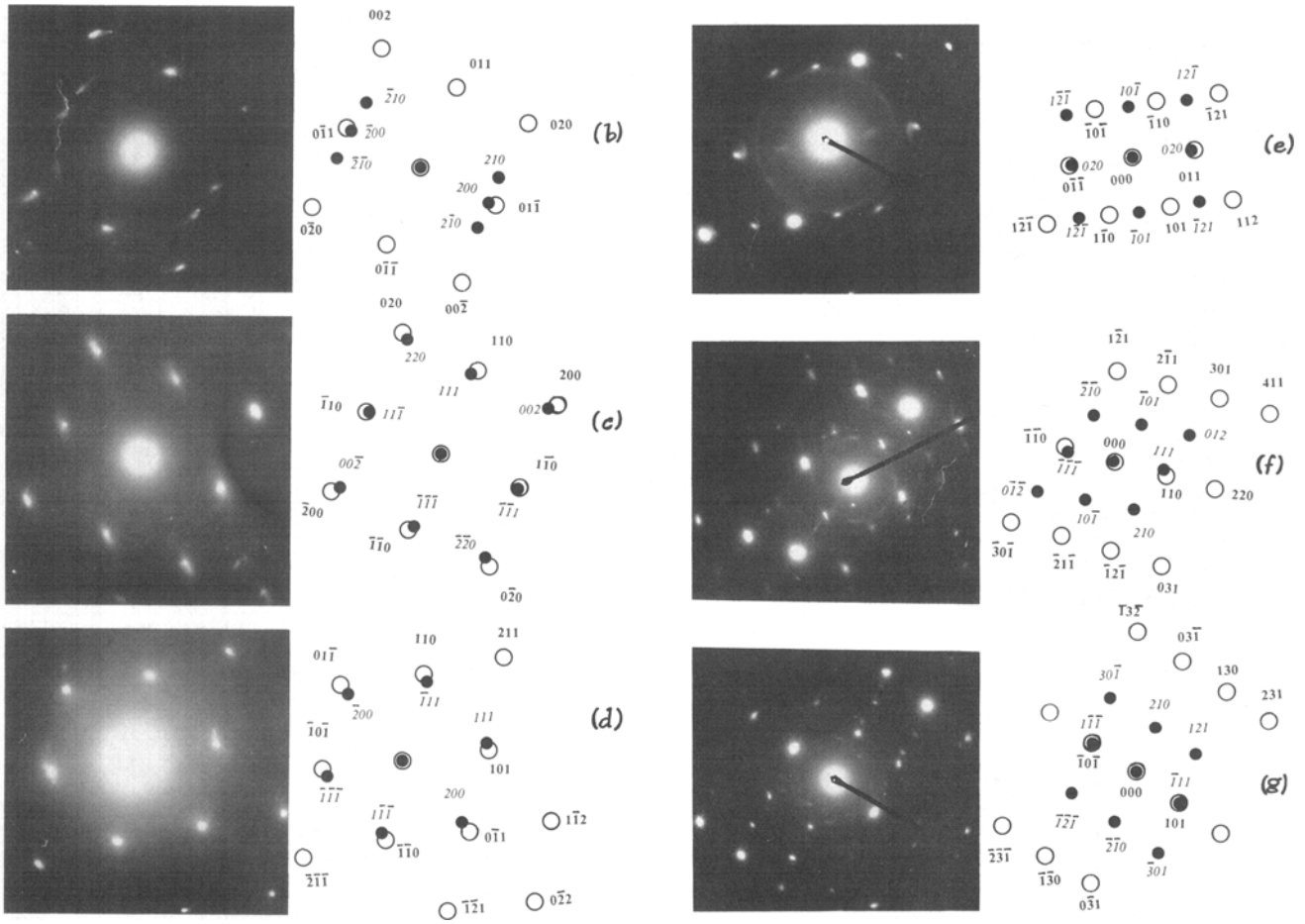

Fig. 5 — Sample tempered up to 450 K. (*a*) Bright-field electron micrograph. Diffraction patterns with corresponding key diagrams of martensite matrix M and orthorhombic carbide, as labeled in the convention of η-carbide by Hirotsu and Nagakura.[8] Beam parallel to (*b*) $[100]_M \parallel [001]_\eta$, (*c*) $[001]_M \parallel [\bar{1}10]_\eta$, (*d*) $[\bar{1}11]_M \parallel [01\bar{1}]_\eta$, (*e*) $[11\bar{1}]_M \parallel [101]_\eta$, (*f*) $[\bar{1}13]_M \parallel [1\bar{2}1]_\eta$, and (*g*) $[\bar{3}13]_M \parallel [\bar{1}23]_\eta$. Spots of matrix M and of η-carbide are labeled as **hkl** and *hkl*, respectively. Double diffraction spots or other variants are not taken into account in the key diagrams.

quality as those presented here for the fully aged martensite. An earlier study[16] revealed the existence of superstructure spots but only those which are separated by a $(1/6)2\mathbf{c}^*$ vector in reciprocal space. The existence of the set of spots separated by $(1/12)2\mathbf{c}^*$ at positions $(h/2, k/2, l)$ already forwarded for a Fe-1.62 wt pct C alloy is here unambiguously confirmed.[10,12]

Before observing that the superlattice spots were, in fact, split, Izotov and Utevskiy[16] proposed a structure Fe_4C with a tetragonal lattice and parameters $a' = a\sqrt{2}$ and $c' = c$, where a and c are parameters of the corresponding axes in martensite. In order to account for the splitting, Nagakura and co-workers[10,12] proposed a long period superstructure along the c-axis with an

orthorhombic lattice with parameters $a' = b' = a\sqrt{2}$ and $c' = 12c$, in which the overall formula of Fe_4C is conserved.

Unfortunately, a most recent atom-probe field-ion microscopy (AP/FIM) study[4] shows that the carbon content lies between 10 and 15 at. pct. This is the reason why Taylor *et al.*[4] instead propose an $Fe_{16}C_2$ structure isomorphous with that of $Fe_{16}N_2$. One cannot share this proposal either, since it would have produced diffraction patterns similar to those observed in the nitrogen iron alloys.

In light of these facts, there is need to cope with the following requirements: keep a $12a$ superperiod along the c-axis as Nagakura and Toyoshima[10] did and stay within the correct range of carbon concentration. Such a solution can be found within the frame of the carbon multiplet model as proposed by Génin.[1,3] The model is based on the relative stability of carbon pair configurations of the C-C $1/2\langle 111\rangle$ and C-C $\langle 101\rangle$ type. If Fe and C atoms are considered to be hard spheres, one notes that the available spacing of 0.39 Å between iron atoms along the c-axis is about one fourth of the diameter of the carbon interstitial (1.54 Å). Thus, it is possible to insert one carbon atom along the c-axis every four iron atoms. However, if one wants to maintain the local environments of the iron atoms as proposed from the Mössbauer spectroscopy study,[1,7] a sequence of carbon and iron atoms, 1C-2Fe-1C-5Fe-1C-5Fe, along the c-axis is arrived at which corresponds to a $12a$ superperiod.[3]

Figures 6(a) and (b) represent such a long periodicity, where (a) shows the $(100)_{\alpha'}$ projection displaying two atom layers and (b) depicts the overall precipitate.[3] The closest carbon distance along the c-axis, which is $(12/5)a$, gives rise to a spot at $(5/12)2\mathbf{c}^*$ and, by double diffraction, to a second spot at $(7/12)2\mathbf{c}^*$. Therefore, one explains the first set of spots corresponding to the $(1/6)2\mathbf{c}^*$ splitting around spots (h, k, l) such that $(h + k + l)$ is odd. The other set of spots, *i.e.*, those corresponding to a splitting $(1/12)2\mathbf{c}^*$ at $(h/2, k/2, l)$ positions, is due to the antiphase character of the structure with the $12a$ overall periodicity. Moreover, the chemical formula corresponding to the precipitate is Fe_6C, which is in good agreement with the AP/FIM result.[4] Figures 7(a) and (b) represent $(100)_{\alpha'}$ and $(010)_{\alpha'}$ projections of the unit cell of the Fe_6C carbide, while Table I gives the reduced coordinates of the Fe and C atoms in the orthorhombic unit cell, where $a' = 2a$, $b' = 3a$, and $c' = 12a$. One notes that the 1C-2Fe-1C-5Fe-1C-5Fe sequence introduces antiphase boundaries along the c-axis, and carbon-rich regions with local composition of 25 at. pct C alternate with carbon-free regions. These later, which are compressed along $[001]_{\alpha'}$, constitute the "κ" or "C" phase reported by Lysak and Vov'k[21] or Chen and Winchell.[22]

Finally, the diffusion-scattering streaks around the fundamental spots come from the platelike shape of the precipitates, as described by Figure 6(b) edge on.[3] The four variants of habit plane are precisely $(023)_{\alpha'}$, $(0\bar{2}3)_{\alpha'}$, $(203)_{\alpha'}$, and $(\bar{2}03)_{\alpha'}$, giving rise to the streaks in the corresponding directions of the reciprocal lattice. This experimental result is remarkably consistent with the prediction made by Khachaturyan from elasticity considerations.[3,19]

One notes also that the sample aged at 330 K for 1 hour displays a diffraction pattern with only streaks (Figure 3(a)), proving that the ordering and long-range superperiod is not yet evolved. This agrees with the kinetics study, which indicates that 350 K must be reached with 1-hour isochronal holdings for ordering. The correlation between Mössbauer spectroscopy and TEM observations is clearly demonstrated.

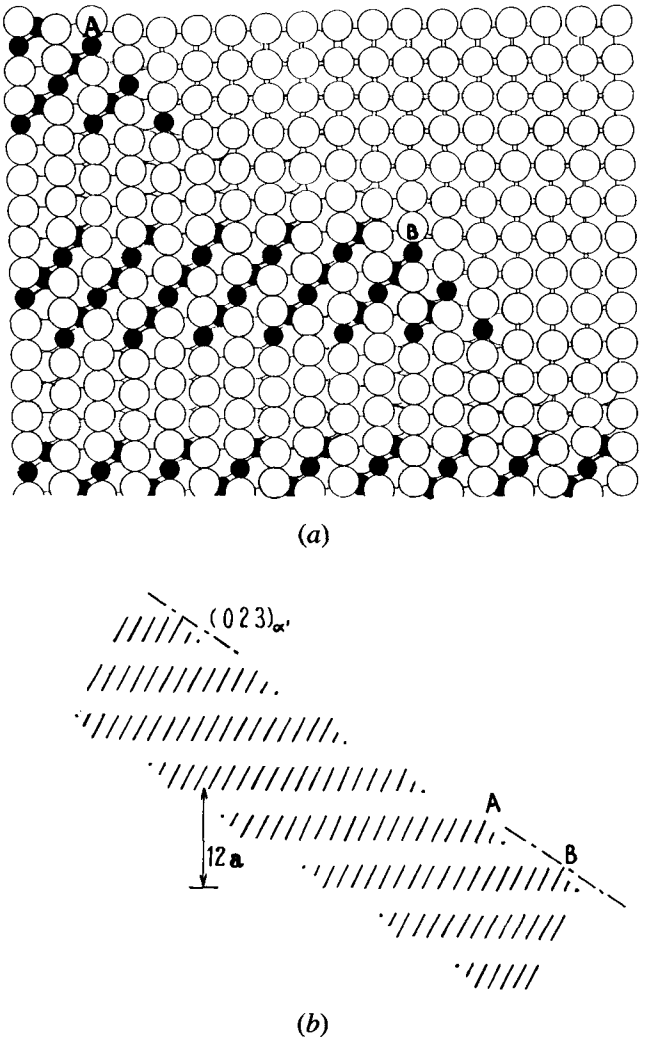

Fig. 6—(*a*) $(100)_{\alpha'}$ projection of extended multiplet, the Fe_6C carbide as proposed by Génin,[3] introducing antiphase domains by alternating 1C, 2Fe, 1C, 5Fe, 1C, and 5Fe sequences of carbon and iron atoms along $[001]_{\alpha'}$. Atomic radii of Fe and C atoms are at scale, and two layers of atoms are represented. Habit plane is $(023)_{\alpha'}$. (*b*) Overall view of the precipitate, showing the domains and the $12a$ periodicity. The streaks in the $[023]_{\alpha'}$ direction symbolize the individual carbon multiplets. The carbon-free regions between the domains correspond to the "C" phase[20] or "κ" phase.[21]

B. *The ε- or η-Carbide Structure*

Jack studied the first stage of tempering and determined that the carbide which is formed corresponds to a hexagonal close-packed (hcp) stacking of iron atoms, with the carbon atoms being inserted within the octahedral sites.[23] Therefore, he gave it the name of ε-carbide. Lattice parameters were determined to be $a_\varepsilon = 2.704$ Å and $c_\varepsilon = 4.383$ Å, and the orientation relationships between the carbon-depleted matrix M, sometimes known

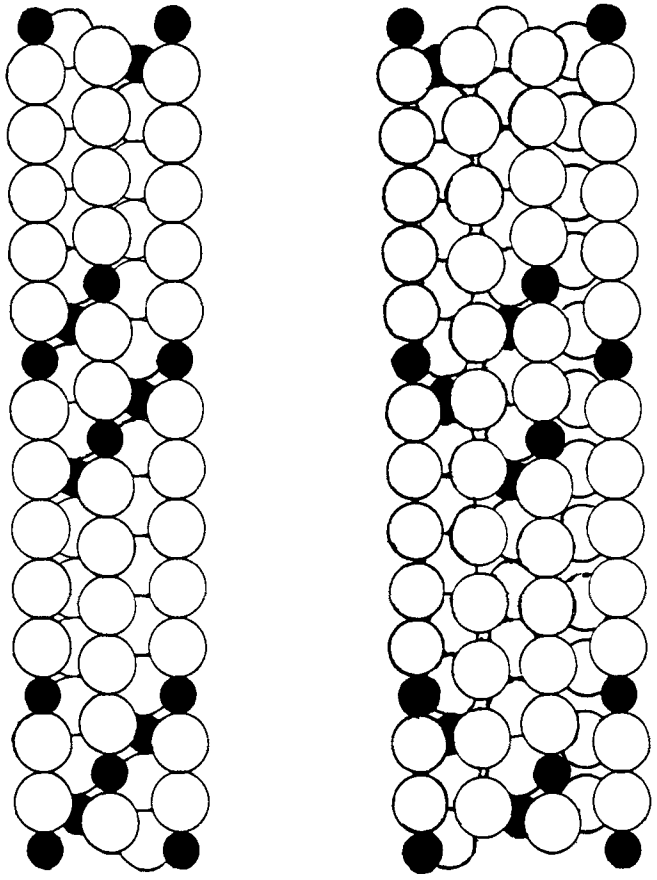

(*a*) (*b*)

Fig. 7—Unit cell of the Fe_6C carbide as proposed by Génin:[3] (*a*) $(100)_\alpha$ and (*b*) $(010)_\alpha$ projections.

as α'', and the carbide were given to be $(10\bar{1}1)_\varepsilon \parallel (101)_M$ and $[0001]_\varepsilon \parallel [011]_M$.

Later, Hirotsu and Nagakura, by studying a 1.13 wt pct C martensite, argued that the carbide is not actually hexagonal but orthorhombic, preferring the name of η-carbide.[8] They proposed for parameters of the unit cell $a_\eta = 4.704$ Å, $b_\eta = 4.318$ Å, $c_\eta = 2.830$ Å. Note that their choice of axes takes b_η to be parallel to c_ε. The orthorhombic structure departs from the hexagonal lattice if the ratio a_η/c_η differs from $\sqrt{3}$. Thus, from their data, a ratio value of 1.662 is obtained. Moreover, it was concluded that the orthorhombic structure is due to the ordering of the carbon interstitials in a way similar to that observed for Co_2N or Co_2C.[8,9] It looked to them as if η-carbide was an ordered form of the ε-carbide. This can be synthesized in the hexagonal form, but the carbide obtained through the tempering of steels would be the ordered orthorhombic η-carbide and the orientation relationships between the matrix M and η-carbide were given to be $(110)_\eta \parallel (010)_M$ and $[001]_\eta \parallel [100]_M$.

From the patterns of Figure 5, it is confirmed that the carbide has an orthorhombic unit cell with an a_η/c_η ratio equal to 1.655. If keeping Hirotsu and Nagakura's nomenclature,[8] lattice parameters are computed to be $a_\eta = 4.694$ Å, $b_\eta = 4.300$ Å, and $c_\eta = 2.837$ Å. Nevertheless, if the orthorhombic character of the unit cell is fully recognized,[8,24,25] as distinct from the hexagonal symmetry advocated in the early studies,[23,26,27] many patterns are presented in order to check whether the ordering of interstitials giving a phase isomorphous with Co_2N is actually the correct one. This ordering would lead to superlattice spots, as recorded in Table I of Reference 8. Some of these spots are lacking in our diffraction patterns, similar to Taylor *et al.*'s observations.[6] For instance, on the $[001]_M \parallel [\bar{1}10]_\eta$ pattern (Figure 5(c)), the superlattice spot labeled $(110)_\eta$ in Reference 8 is absent here as well as in Reference 6. In Reference 24, this spot is not much visible either, while Shimizu and Okamoto[24] observed it but attributed it to originate probably from another diffracting carbide variant. Even in an earlier TEM study, Murphy and Whiteman[27] display no such spots in any of their $\langle 100\rangle_M$ patterns. On the contrary, a $(012)_\eta$ spot is observed here in the $[\bar{1}13]_M \parallel [1\bar{2}1]_\eta$ pattern (Figure 5(f)), which is not present in Reference 8. From these experimental facts, one can infer that η-carbide is most likely not isomorphous with Co_2N. All results are gathered in Table II, where some of the interplanar spacings can be compared between the computed and observed values.

Another type of ordering has been proposed by Génin[1,3] based on the assumption that there exists an *in situ* transformation of the extended multiplets into the ε- or η-carbide precipitates. Figure 5(a), which displays the morphology of the precipitated structure of the ε- or η-carbide precipitation, is very similar indeed to the tweed structure obtained by aging (Figures 3(a) and 4(e)). The major differences are that the precipitates are coarser after tempering and that the habit plane is now close to $\{102\}_M$ instead of $\{203\}_M$. This fact has been most precisely established by Taylor *et al.*[6]

The *in situ* transformation is well illustrated in Figure 8. The carbon atoms rearrange themselves from a carbon-rich region inside the multiplet to the ε- or η-carbide. Reference 1 offers the explanation for the mechanism through which such a transformation could occur. It is deduced that the ε- or η-carbide should correspond to an ordered phase, as illustrated in Figure 8(c), and to the formula Fe_9C_4,[3] *i.e.*, $Fe_{2.25}C$, which is close indeed to the experimental $Fe_{2.4}C$.[7,28–30] If considered in a hexagonal Fe sublattice, the carbon ordering would be trigonal. Therefore, the unambiguous orthorhombic character of the structure of the precipitated carbide can only originate from the elastic distortions due to its coherency with the tetragonal matrix. This can also explain the slight discrepancies which are observed in the lattice parameters if one compares the different studies,[6,8,9,24,25] and the orthorhombic character certainly depends on the composition and on the level of tempering of a given martensite.

C. *Comments about the Fe_6C Structure*

In a Reply[32] to a Discussion[31] of the paper quoted here,[4] G.B. Olson *et al.* state recently that "Génin's Fe_6C structure does not correspond to any known transition metal carbide or nitride structure and involves C atoms which are closely spaced as the Fe-Fe near-neighbor distance of 2.5 Å. This is much closer than the smallest C-C distance of 3.09 Å in the known θ-Fe_3C cementite structure or the smallest nitrogen-nitrogen (N-N) distance in the known α''-$Fe_{16}N_2$ and γ'-Fe_4N structures."

Table I. Reduced Coordinates of Carbon and Iron Atoms in the $2a \times 3a \times 12a$ Unit Cell of the Fe_6C Carbide Due to the Clustering and Long-Range Ordering[3]*

Atoms	x	y	z					
Fe	0	0	0.058	0.131	0.248	0.320	0.392	0.464
			0.536	0.653	0.725	0.797	0.869	0.942
C	0	0	0	0.189	0.595	—	—	—
Fe	0.5	0	0.036	0.153	0.225	0.297	0.369	0.442
			0.559	0.631	0.748	0.820	0.892	0.964
C	0.5	0	0.095	0.5	0.689	—	—	—
Fe	0.25	0.167	0.106	0.178	0.25	0.322	0.394	0.511
			0.583	0.7	0.772	0.845	0.917	0.989
C	0.25	0.167	0.047	0.453	0.642	—	—	—
Fe	0.75	0.167	0.011	0.083	0.2	0.272	0.345	0.417
			0.488	0.606	0.678	0.75	0.822	0.894
C	0.75	0.167	0.142	0.547	0.953	—	—	—
Fe	0	0.333	0.042	0.125	0.208	0.292	0.375	0.458
			0.542	0.625	0.708	0.792	0.875	0.958
Fe	0.5	0.333	0.042	0.125	0.208	0.292	0.375	0.458
			0.542	0.625	0.708	0.792	0.875	0.958
Fe	0.25	0.5	0.011	0.083	0.2	0.272	0.345	0.417
			0.488	0.606	0.678	0.75	0.822	0.894
C	0.25	0.5	0.142	0.547	0.953	—	—	—
Fe	0.75	0.5	0.106	0.178	0.25	0.322	0.394	0.511
			0.583	0.7	0.772	0.845	0.917	0.989
C	0.75	0.5	0.047	0.453	0.642	—	—	—
Fe	0	0.667	0.036	0.153	0.225	0.297	0.369	0.442
			0.559	0.631	0.748	0.820	0.892	0.964
C	0	0.667	0.095	0.5	0.689	—	—	—
Fe	0.5	0.667	0.058	0.131	0.248	0.320	0.392	0.464
			0.536	0.653	0.725	0.797	0.869	0.942
C	0.5	0.667	0	0.189	0.595	—	—	—
Fe	0.25	0.833	0.042	0.125	0.208	0.292	0.375	0.458
			0.542	0.625	0.708	0.792	0.875	0.958
Fe	0.75	0.833	0.042	0.125	0.208	0.292	0.375	0.458
			0.542	0.625	0.708	0.792	0.875	0.958

*Atomic radii of iron and carbon are 1.24 and 0.77 Å, respectively; a is 2.865 Å. Actual positions can be slightly off predicted positions, but the 1C-2Fe-1C-5Fe-1C-5Fe sequence is conserved (Figure 7).

The argument seems odd when considering the well-known ε iron carbide or nitride, where the C-C or N-N distances are about 2.7 Å.

Later on, it is also stated that "with such dense clustering of C atoms, they are many Fe atoms with more than one C first neighbor." As clearly explained in Reference 1, most iron atoms in Fe_6C have two carbon first nearest-neighbors which correspond to component D in the Mössbauer spectra of the aged martensites. The hyperfine field of 262 kOe then observed[1] is typical of iron atoms with two carbon neighbors. It compares favorably with values of hyperfine fields found for homologous iron atoms with two carbon neighbors in ε- or η-carbide, as compiled in Table IV of Reference 7. In that study,[7] the values obtained for the D component of Fe_6C lie in the range of 261 to 266 kOe, whereas those for the G component of ε- or η-carbide lie in the range of 268 to 277 kOe. Therefore, the preliminary electronic calculations by Krasko are consistent with the hyperfine magnetic fields measured by Mössbauer spectroscopy of aged martensites.[1,7]

Finally, we would emphasize that the *M_s temperatures of Fe-C martensites with high carbon content are below the ambient*, as reported in Table I of Reference 7. Such martensites will not be aged before any measurements can be made.[1,7]

Table II. Interplanar Spacings of the Diffraction Spots Found in the Patterns of Figure 5*

Phase	Plane *hkl*	Interplanar Spacings (Å) $d_{hkl_{exp}}$	$d_{hkl_{theor}}$[8]
Orthorhombic η-carbide			
	101	2.44	2.42
	011	2.37	2.37
	200	2.35	2.35
	020	2.16	2.16
	111	2.13	2.11
	210	2.06	2.06
	121	1.61	1.61
	220	1.59	1.59
	301	1.37	1.37
	012	1.34	1.34
	212	1.17	1.17

*The (*hkl*) indices are labeled in the η-carbide nomenclature proposed by Hirotsu and Nagakura.[8]

V. CONCLUSIONS

The TEM study of the structural transformations obtained by aging high-carbon 1.95 wt pct C iron

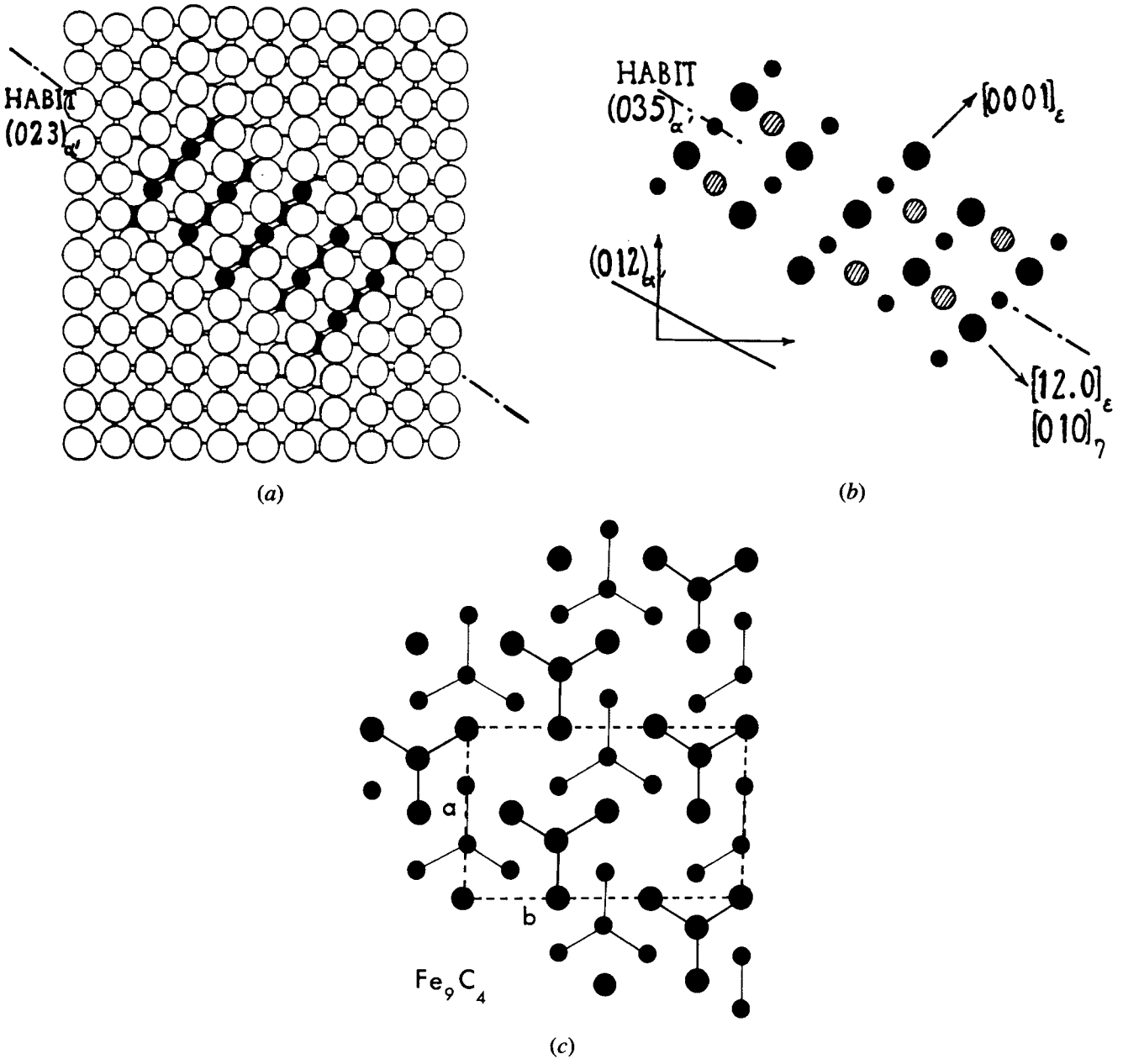

Fig. 8—The *in situ* transformation of an extended multiplet into the ε- or η-carbide. (*a*) $(100)_{\alpha'}$ projection of an extended multiplet embedded in the matrix. Atomic radii of Fe and C atoms are at scale, and two layers of atoms are represented. (*b*) $(100)_{\alpha'}$ projection of a small Fe_9C_4 ε- or η-carbide after the transformation. Hatched circles are carbon atoms added to the extended multiplet during the transformation. Three layers of carbon atoms are represented. Habit plane is close to $(012)_{\alpha'}$. (*c*) $(0001)_{\varepsilon}$ or $(010)_{\eta}$ projection of two adjacent layers of carbon atoms in the perfectly ordered Fe_9C_4 ε- or η-carbide, as advocated by Génin.[3]

martensites correlates with the Mössbauer spectroscopy study of the kinetics.[7] The two steps of aging, then attributed to the clustering and ordering of carbon interstitials, are clearly distinguishable. Electron diffraction patterns of samples aged isochronally for 1 hour up to 57 °C display only streaks in $\langle 203 \rangle^*$ directions, which correspond to the four orientation variants of the precipitates; these variants together constitute the tweedlike structure modulation when only clustering has occurred. Patterns of samples aged at 79 °C for 2 hours show, in addition to the streaks, two sets of superstructure spots, a $(1/6)2\mathbf{c}^*$ splitting about (h, k, l) reflections with $(h + k + l)$ odd and a $(1/12)2\mathbf{c}^*$ splitting about $(h/2, k/2, l)$ reflections when ordering has occurred.

The four $\{203\}_{\alpha'}$ habit plane variants and the superstructure spots are explained by alternating 1C, 2Fe, 1C, 5Fe, 1C, and 5Fe sequences of carbon and iron atoms along the tetragonal axis, which leads to platelike precipitates of overall formula Fe_6C. This sequence introduces along this axis antiphase domains and alternating carbon-rich and carbon-depleted regions. These later constitute the "κ" or "C" phase.[21,22]

The first stage of tempering which follows the ordering step is characterized by the *in situ* transformation of the previous carbide precipitates, *i.e.*, the extended multiplets, to ε- or η-carbide, as evidenced by the tweedlike structure which strongly resembles the structure obtained by aging except for the habit plane, which is now of the

$\{102\}_M$ type.[6] The carbide is unambiguously orthorhombic, but no evidence of the ordering of the interstitials as proposed by Hirotsu and Nagakura[8] is observed. Therefore, the departure from the hexagonal symmetry is likely due to the coherency of the platelike precipitate within the stretched matrix. Consistent with the carbon multiplet model, the ε- or η-carbide with Fe_9C_4 stoichiometry[1,3] close to the experimental $Fe_{2.4}C$ is advocated.

REFERENCES

1. J.-M.R. Génin: *Metall. Trans. A*, 1987, vol. 18A, pp. 1371-88.
2. E.J. Mittemeijer, L. Cheng, P.J. van der Schaff, C.M. Brakman, and B.M. Korevaar: *Metall. Trans. A*, 1988, vol. 19A, pp. 925-32.
3. J.-M.R. Génin: *Metall. Trans. A*, 1988, vol. 19A, pp. 2901-09.
4. K.A. Taylor, L. Chang, G.B. Olson, G.D.W. Smith, M. Cohen, and J.B. VanderSande: *Metall. Trans. A*, 1989, vol. 20A, pp. 2717-37.
5. K.A. Taylor, G.B. Olson, M. Cohen, and J.B. VanderSande: *Metall. Trans. A*, 1989, vol. 20A, pp. 2739-47.
6. K.A. Taylor, G.B. Olson, M. Cohen, and J.B. VanderSande: *Metall. Trans. A*, 1989, vol. 20A, pp. 2749-65.
7. O.N.C. Uwakweh, J. Ph. Bauer, and J.-M.R. Génin: *Metall. Trans. A*, 1990, vol. 21A, pp. 589-602.
8. Y. Hirotsu and S. Nagakura: *Acta Metall.*, 1972, vol. 20, pp. 645-55.
9. Y. Hirotsu and S. Nagakura: *Trans. Jpn. Inst. Met.*, 1974, vol. 15, pp. 129-34.
10. S. Nagakura and M. Toyoshima: *Trans. Jpn. Inst. Met.*, 1979, vol. 20, pp. 100-10.
11. M. Kusunoki (née Toyoshima) and S. Nagakura: *J. Appl. Crystallogr.*, 1981, vol. 15, pp. 513-17.
12. S. Nagakura, Y. Hirotsu, M. Kusunoki-Toyoshima, T. Suzuki, and Y. Nakamura: *Metall. Trans. A*, 1983, vol. 14A, pp. 1025-31.
13. R.F. Mehl and D.M. Van Winkle: *Rev. Métall.*, 1953, vol. 50, p. 465.
14. M. Oka and C.M. Wayman: *Trans. AIME*, 1968, vol. 242, pp. 337-38; *Trans. ASM*, 1969, vol. 62, pp. 370-76.
15. S.H. Wen, E. Kostlan, H. Hong, A.G. Khachaturyan, and J.W. Morris, Jr.: *Acta Metall.*, 1981, vol. 29, pp. 1247-54.
16. V.I. Izotov and L.M. Utevskiy: *Fiz. Met. Metalloved.*, 1967, vol. 25, pp. 98-110.
17. A.G. Khachaturyan and T.A. Onisimova: *Fiz. Met. Metalloved.*, 1968, vol. 25, pp. 973-80.
18. P. Grégoire, P. Pahuta, C. Dagbert, J. Galland, and H. Hyspecka: *Proc. ICOMAT 85*, Japan Institute of Metals, Nara, Japan, 1986, pp. 401-05.
19. A.G. Khachaturyan: *Theory of Structural Transformation in Solids*, John Wiley & Sons, New York, NY, 1983.
20. V.I. Izotov and L.M. Utevskiy: *Fiz. Met. Metalloved.*, 1968, vol. 25, pp. 86-95.
21. L.I. Lysak and Y.N. Vov'k: *Fiz. Met. Metalloved.*, 1965, vol. 19, pp. 699-706; vol. 20, pp. 540-54.
22. P.C. Chen and P.G. Winchell: *Metall. Trans. A*, 1980, vol. 11A, pp. 1333-39.
23. K.H. Jack: *J. Iron Steel Inst.*, 1951, vol. 169, pp. 26-36.
24. K. Shimizu and H. Okamoto: *Trans. Jpn. Inst. Met.*, 1974, vol. 15, pp. 193-99.
25. D.L. Williamson, K. Nakazawa, and G. Krauss: *Metall. Trans. A*, 1979, vol. 10A, pp. 1351-63.
26. M.G.H. Wells: *Acta Metall.*, 1964, vol. 12, pp. 389-99.
27. Samuel Murphy and John Anthony Whiteman: *Metall. Trans.*, 1970, vol. 1, pp. 843-48.
28. B.S. Lement: *Trans. ASM*, 1953, vol. 45, pp. 597-98.
29. M.P. Arbuzov and B.V. Khayenko: *Fiz. Met. Metalloved.*, 1962, vol. 13, pp. 686-92.
30. R. Ruhl and M. Cohen: *Trans. TMS-AIME*, 1969, vol. 245, pp. 241-51.
31. J.-M.R. Génin: *Metall. Trans. A*, 1990, vol. 21A, pp. 2083-86.
32. G.B. Olson, K.A. Taylor, and M. Cohen: *Metall. Trans. A*, 1990, vol. 21A, p. 2086.